

Adaptive Cross Tubal Tensor Approximation

Salman Ahmadi-Asl^a, Anh Huy Phan^a, Andrzej Cichocki^{a,b}, Anastasia Sozykina^a, Zaher Al Aghbari^c, Jun Wang^a, and Ivan Oseledets^a

^a*Center for Artificial Intelligence Technology, Skolkovo Institute of Science and Technology, Moscow, Russia, s.asl@skoltech.ru,*

^b*Systems Research Institute of Polish Academy of Science, Warsaw, Poland,*

^c*Department of Computer Science, University of Sharjah, Sharjah, 27272, UAE,*

Abstract

In this paper, we propose a new adaptive cross algorithm for computing a low tubal rank approximation of third-order tensors, with less memory and lower computational complexity than the truncated tensor SVD (t-SVD). This makes it applicable for decomposing large-scale tensors. We conduct numerical experiments on synthetic and real-world datasets to confirm the efficiency and feasibility of the proposed algorithm. The simulation results show more than one order of magnitude acceleration in the computation of low tubal rank (t-SVD) for large-scale tensors. An application to pedestrian attribute recognition is also presented.

Keywords: Cross tensor approximation, tensor SVD, tubal product

2000 MSC: 15A69, 46N40, 15A23

1. Introduction

Tensors are high-dimensional generalizations of matrices and vectors. Contrary to the rank of matrices, the rank of tensors is not well understood and has to be defined and determined. Different types of tensor decompositions can have different rank definitions such as Tensor Train (TT) [1], Tucker decomposition [2] and its special case, i.e. Higher Order SVD (HOSVD) [3], CANDECOMP/PARAFAC decomposition (CPD) [4, 5], Block Term decomposition [6], Tensor Train/Tensor Ring (TT-TR) decomposition [1, 7, 8], tubal SVD (t-SVD) [9]. The t-SVD factorizes a tensor into three tensors, two orthogonal tensors and one f-diagonal tensor (to be discussed in Section 3). Like the SVD for matrices, the truncation version of the t-SVD provides the best tubal rank approximation for every unitary invariant tensor norm. The t-SVD has been successfully applied in

deep learning [10, 11], tensor completion [12, 13], image reconstruction [14] and tensor compression [15].

Decomposing big data tensors into the t-SVD format is a challenging task, especially when the data is extremely massive and we can not view the entire data tensor. The cross, skeleton, or CUR approximation is a useful paradigm widely used for fast low-rank matrix approximation. Achieving a higher compression ratio, and problems with data interpretation are other motivations to use the cross approximation methods. The main feature of the cross algorithms that makes them effective for managing very large-scale data tensors is their ability to use less memory and have lower computational complexity. When it comes to the higher compression capacity, for instance, the cross matrix approximation provides sparse factor matrices, whereas the SVD of sparse matrices fails to do so, resulting in a more compact data structure. It is also known that the cross approximations can provide more interpretable approximations, we refer to [16] for more details.

Due to the mentioned motivations, the cross matrix approximation [17, 18] has been generalized to different types of tensor decompositions such as the TT-Cross [19], Cross-3D [20], FSTD [21], and tubal Cross [22]. The cross matrix approximation is generalized to the tensor case based on the tubal product (t-product) in [22] where some individual lateral and horizontal slices are selected and based on them a low tubal rank approximation is computed. The main drawback of this approach is its dependency on the tubal rank estimation, which may be a difficult task in real-world applications. To tackle this problem, we propose to generalize the adaptive cross matrix approximation [23, 24, 25] to tensors based on the t-product. The idea is to select one actual lateral slice and one actual horizontal slice at each iteration and adaptively check the tubal rank of the tensor.

The generalization of the adaptive cross matrix approximation to tensors based on the t-product is an interesting problem and in this paper, we discuss how to perform it properly. The novelties done in this work include:

- A new adaptive tubal tensor approximation algorithm, which estimates the tubal rank and compute the low tubal rank approximation. The proposed algorithm does not need to use the whole data tensor and at each iteration works only on a part of the horizontal and lateral slices. This facilitates handling large-scale tensors.
- Presenting an application in pedestrian attribute recognition.

The rest of the paper is structured as follows. The basic definitions are given

in Section 2. The t-SVD model is introduced in Section 3. The cross matrix approximation and its adaptive version are discussed in Section 4. Section 5, shows how to generalize the adaptive cross approximation to the tensor case based on the t-product. We compare the computational complexity of the algorithms in Section 6. The experimental results are presented in Section 7 and Section 8 concludes the paper and presents potential future directions.

2. Preliminaries

The key notations and concepts used in the rest of the paper are introduced in this section. A tensor, a matrix and a vector are denoted by an underlined bold capital case letter, a bold capital case letter and a bold lower case letter, respectively. Slices are subtensors generated with fixed all but two modes. Our work is for real-valued third-order tensors but generalization to complex higher order tensor is also straightforward. For a third-order tensor, $\underline{\mathbf{X}}$, the three types of slices $\underline{\mathbf{X}}(:, :, k)$, $\underline{\mathbf{X}}(:, j, :)$, $\underline{\mathbf{X}}(i, :, :)$ are called frontal, lateral and horizontal slices. For a third-order tensor $\underline{\mathbf{X}}$, the three types fibers $\underline{\mathbf{X}}(:, j, k)$, $\underline{\mathbf{X}}(i, :, k)$, $\underline{\mathbf{X}}(i, j, :)$ are called columns, rows and tubes. The notation “conj” means the complex conjugate of all elements (complex numbers) of a matrix. The notations $\mathbf{X}_{(:, -j)}$ and $\mathbf{X}_{(-i, :)}$ are used to denote new sub-matrices of the matrix \mathbf{X} with the j -column and the i -th row removed. The Frobenius norm of tensors/matrices is denoted by $\|\cdot\|_F$ and the Euclidean norm of a vector is shown by $\|\cdot\|_2$. The notation $|\cdot|$ stands for the absolute value of a real number. We need the subsequent definitions to introduce the tensor SVD (t-SVD) model.

Definition 1. (t-product) Let $\underline{\mathbf{X}} \in \mathbb{R}^{I_1 \times I_2 \times I_3}$ and $\underline{\mathbf{Y}} \in \mathbb{R}^{I_2 \times I_4 \times I_3}$, the t-product $\underline{\mathbf{X}} * \underline{\mathbf{Y}} \in \mathbb{R}^{I_1 \times I_4 \times I_3}$ is defined as follows

$$\underline{\mathbf{C}} = \underline{\mathbf{X}} * \underline{\mathbf{Y}} = \text{fold}(\text{circ}(\underline{\mathbf{X}}) \text{unfold}(\underline{\mathbf{Y}})), \quad (1)$$

where

$$\text{circ}(\underline{\mathbf{X}}) = \begin{bmatrix} \mathbf{X}^{(1)} & \mathbf{X}^{(I_3)} & \dots & \mathbf{X}^{(2)} \\ \mathbf{X}^{(2)} & \mathbf{X}^{(1)} & \dots & \mathbf{X}^{(3)} \\ \vdots & \vdots & \ddots & \vdots \\ \mathbf{X}^{(I_3)} & \mathbf{X}^{(I_3-1)} & \dots & \mathbf{X}^{(1)} \end{bmatrix},$$

and

$$\text{unfold}(\underline{\mathbf{Y}}) = \begin{bmatrix} \mathbf{Y}^{(1)} \\ \mathbf{Y}^{(2)} \\ \vdots \\ \mathbf{Y}^{(I_3)} \end{bmatrix}, \quad \underline{\mathbf{Y}} = \text{fold}(\text{unfold}(\underline{\mathbf{Y}})).$$

Here, $\mathbf{X}^{(i)} = \underline{\mathbf{X}}(:, :, i)$ and $\mathbf{Y}^{(i)} = \underline{\mathbf{Y}}(:, :, i)$ for $i = 1, 2, \dots, I_3$.

We denote by $\widehat{\underline{\mathbf{X}}}$, the Fourier transform of $\underline{\mathbf{X}}$ along its third mode, which can be computed as $\widehat{\underline{\mathbf{X}}} = \text{fft}(\underline{\mathbf{X}}, [], 3)$. It is known that the block circulant matrix, $\text{circ}(\underline{\mathbf{X}}) \in \mathbb{R}^{I_1 I_3 \times I_2 I_3}$, can be block diagonalized, i.e.,

$$(\mathbf{F}_{I_3} \otimes \mathbf{I}_{I_1}) \text{circ}(\underline{\mathbf{X}}) (\mathbf{F}_{I_3}^{-1} \otimes \mathbf{I}_{I_2}) = \widehat{\underline{\mathbf{X}}}, \quad (2)$$

where $\mathbf{F}_{I_3} \in \mathbb{R}^{I_3 \times I_3}$ is the discrete Fourier transform matrix and $(\mathbf{F}_{I_3} \otimes \mathbf{I}_{I_1})/\sqrt{I_3}$ is a unitary matrix. Here, the block diagonal matrix $\widehat{\underline{\mathbf{X}}}$ is

$$\widehat{\underline{\mathbf{X}}} = \begin{bmatrix} \widehat{\underline{\mathbf{X}}}(:, :, 1) & & & \\ & \widehat{\underline{\mathbf{X}}}(:, :, 2) & & \\ & & \ddots & \\ & & & \widehat{\underline{\mathbf{X}}}(:, :, I_3) \end{bmatrix}, \quad (3)$$

and we have the following important properties [26, 27]

$$\widehat{\underline{\mathbf{X}}}(:, :, 1) \in \mathbb{R}^{I_1 \times I_2}, \quad (4)$$

$$\text{conj}(\widehat{\underline{\mathbf{X}}}(:, :, i)) = \widehat{\underline{\mathbf{X}}}(:, :, I_3 - i + 2), \quad (5)$$

for $i = 2, \dots, \lceil \frac{I_3+1}{2} \rceil + 1$. The t-product can be equivalently performed in the Fourier domain. Indeed, let $\underline{\mathbf{C}} = \underline{\mathbf{X}} * \underline{\mathbf{Y}}$, then from the definition of the t-product and the fact that the block circulant matrix can be block diagonalized, we have

$$\begin{aligned} \text{unfold}(\underline{\mathbf{C}}) &= \text{circ}(\underline{\mathbf{X}}) \text{unfold}(\underline{\mathbf{Y}}) \\ &= (\mathbf{F}_{I_3}^{-1} \otimes \mathbf{I}_{I_1}) ((\mathbf{F}_{I_3} \otimes \mathbf{I}_{I_1}) \text{circ}(\underline{\mathbf{X}}) (\mathbf{F}_{I_3}^{-1} \otimes \mathbf{I}_{I_2})) \\ &\quad ((\mathbf{F}_{I_3}^{-1} \otimes \mathbf{I}_{I_2}) \text{unfold}(\underline{\mathbf{Y}})) \\ &= (\mathbf{F}_{I_3} \otimes \mathbf{I}_{I_1}) \widehat{\underline{\mathbf{X}}} \text{unfold}(\widehat{\underline{\mathbf{Y}}}), \end{aligned} \quad (6)$$

where $\widehat{\underline{\mathbf{Y}}} = \text{fft}(\underline{\mathbf{Y}}, [], 3)$. If we multiply both sides of (6) from the left-hand side with $(\mathbf{F}_{I_3} \otimes \mathbf{I}_{I_1})$, we get $\text{unfold}(\widehat{\underline{\mathbf{C}}}) = \widehat{\underline{\mathbf{X}}} \text{unfold}(\widehat{\underline{\mathbf{Y}}})$, where $\widehat{\underline{\mathbf{C}}} = \text{fft}(\underline{\mathbf{C}}, [], 3)$. This means that $\widehat{\underline{\mathbf{C}}}(:, :, i) = \widehat{\underline{\mathbf{X}}}(:, :, i) \widehat{\underline{\mathbf{Y}}}(:, :, i)$. So, it suffices to transform two given tensors into the Fourier domain and multiply their frontal slices. Then, the resulting tensor in the Fourier domain returned back to the original space via the inverse FFT. Note that due to the equations in (4)-(5), half of the computations are reduced. This procedure is summarized in Algorithm 1.

Definition 2. (Transpose) The transpose of a tensor $\underline{\mathbf{X}} \in \mathbb{R}^{I_1 \times I_2 \times I_3}$ is denoted by $\underline{\mathbf{X}}^T \in \mathbb{R}^{I_2 \times I_1 \times I_3}$ produced by applying the transpose to all frontal slices of the tensor $\underline{\mathbf{X}}$ and reversing the order of the second until the last transposed frontal slices.

Definition 3. (Identity tensor) Identity tensor $\underline{\mathbf{I}} \in \mathbb{R}^{I_1 \times I_1 \times I_3}$ is a tensor whose first frontal slice is an identity matrix of size $I_1 \times I_1$ and all other frontal slices are zero. It is easy to show $\underline{\mathbf{I}} * \underline{\mathbf{X}} = \underline{\mathbf{X}}$ and $\underline{\mathbf{X}} * \underline{\mathbf{I}} = \underline{\mathbf{X}}$ for all tensors of conforming sizes.

Definition 4. (Orthogonal tensor) A tensor $\underline{\mathbf{X}} \in \mathbb{R}^{I_1 \times I_1 \times I_3}$ is orthogonal (under t-product operator) if $\underline{\mathbf{X}}^T * \underline{\mathbf{X}} = \underline{\mathbf{X}} * \underline{\mathbf{X}}^T = \underline{\mathbf{I}}$.

Definition 5. (f-diagonal tensor) If all frontal slices of a tensor are diagonal then the tensor is called an f-diagonal tensor.

Definition 6. (Inverse of a tensor) The inverse of a tensor $\underline{\mathbf{X}} \in \mathbb{R}^{I_1 \times I_1 \times I_3}$ is denoted by $\underline{\mathbf{X}}^{-1} \in \mathbb{R}^{I_1 \times I_1 \times I_3}$ is a unique tensor satisfying $\underline{\mathbf{X}} * \underline{\mathbf{X}}^{-1} = \underline{\mathbf{X}}^{-1} * \underline{\mathbf{X}} = \underline{\mathbf{I}}$, where $\underline{\mathbf{I}} \in \mathbb{R}^{I_1 \times I_1 \times I_3}$ is the identity tensor. The inverse of a tensor can also be computed in the Fourier domain and described in Algorithm 2. The MATLAB command “inv” in Line 3 computes the inverse of a matrix. The Moore–Penrose (MP) inverse of a tensor $\underline{\mathbf{X}} \in \mathbb{R}^{I_1 \times I_2 \times I_3}$ is denoted by $\underline{\mathbf{X}}^\dagger \in \mathbb{R}^{I_2 \times I_1 \times I_3}$ and can be computed by Algorithm 2 where “inv” is replaced with the MATLAB function “pinv”. Here, “pinv” stands for the MP inverse of a matrix.

3. Tensor SVD (t-SVD)

The tensor SVD (t-SVD) represents a tensor as the t-product of three tensors. The first and last tensors are orthogonal, while the middle tensor is an f-diagonal tensor. To be more precise, let $\underline{\mathbf{X}} \in \mathbb{R}^{I_1 \times I_2 \times I_3}$, then the t-SVD of the tensor $\underline{\mathbf{X}}$, is $\underline{\mathbf{X}} = \underline{\mathbf{U}} * \underline{\mathbf{S}} * \underline{\mathbf{V}}^T$, where $\underline{\mathbf{U}} \in \mathbb{R}^{I_1 \times R \times I_3}$, and $\underline{\mathbf{V}} \in \mathbb{R}^{I_2 \times R \times I_3}$ are orthogonal tensors and the tensor $\underline{\mathbf{S}} \in \mathbb{R}^{R \times R \times I_3}$ is f-diagonal [9, 28], see Figure 1 for an illustration on the t-SVD and its truncated version. Note that Algorithm 3 only needs the truncated SVD of the $\lceil \frac{I_3+1}{2} \rceil$ first frontal slices. The generalization of the t-SVD to tensors of order higher than three is done in [29]. Other types of classical matrix decompositions such as QR and LU decompositions can be generalized based on the t-product in straightforward ways.

The computational complexity of Algorithm 3 is dominated by the FFT of all tubes of an input tensor and also the truncated SVD of the frontal slices in

Algorithm 1: Fast t-product of two tensors [9, 27]

Input : Two data tensors $\underline{\mathbf{X}} \in \mathbb{R}^{I_1 \times I_2 \times I_3}$, $\underline{\mathbf{Y}} \in \mathbb{R}^{I_2 \times I_4 \times I_3}$
Output: t-product $\underline{\mathbf{C}} = \underline{\mathbf{X}} * \underline{\mathbf{Y}} \in \mathbb{R}^{I_1 \times I_4 \times I_3}$

- 1 $\widehat{\underline{\mathbf{X}}} = \text{fft}(\underline{\mathbf{X}}, [], 3)$;
- 2 $\widehat{\underline{\mathbf{Y}}} = \text{fft}(\underline{\mathbf{Y}}, [], 3)$;
- 3 **for** $i = 1, 2, \dots, \lceil \frac{I_3+1}{2} \rceil$ **do**
- 4 | $\widehat{\underline{\mathbf{C}}}(:, :, i) = \widehat{\underline{\mathbf{X}}}(:, :, i) \widehat{\underline{\mathbf{Y}}}(:, :, i)$;
- 5 **end**
- 6 **for** $i = \lceil \frac{I_3+1}{2} \rceil + 1, \dots, I_3$ **do**
- 7 | $\widehat{\underline{\mathbf{C}}}(:, :, i) = \text{conj}(\widehat{\underline{\mathbf{C}}}(:, :, I_3 - i + 2))$;
- 8 **end**
- 9 $\underline{\mathbf{C}} = \text{ifft}(\widehat{\underline{\mathbf{C}}}, [], 3)$;

Algorithm 2: Fast inverse computation of the tensor $\underline{\mathbf{X}}$

Input : The data tensor $\underline{\mathbf{X}} \in \mathbb{R}^{I_1 \times I_1 \times I_3}$
Output: Tensor inverse $\underline{\mathbf{X}}^{-1} \in \mathbb{R}^{I_1 \times I_1 \times I_3}$

- 1 $\widehat{\underline{\mathbf{X}}} = \text{fft}(\underline{\mathbf{X}}, [], 3)$;
- 2 **for** $i = 1, 2, \dots, \lceil \frac{I_3+1}{2} \rceil$ **do**
- 3 | $\widehat{\underline{\mathbf{C}}}(:, :, i) = \text{inv}(\widehat{\underline{\mathbf{X}}}(:, :, i))$;
- 4 **end**
- 5 **for** $i = \lceil \frac{I_3+1}{2} \rceil + 1, \dots, I_3$ **do**
- 6 | $\widehat{\underline{\mathbf{C}}}(:, :, i) = \text{conj}(\widehat{\underline{\mathbf{C}}}(:, :, I_3 - i + 2))$;
- 7 **end**
- 8 $\underline{\mathbf{X}}^{-1} = \text{ifft}(\widehat{\underline{\mathbf{C}}}, [], 3)$;

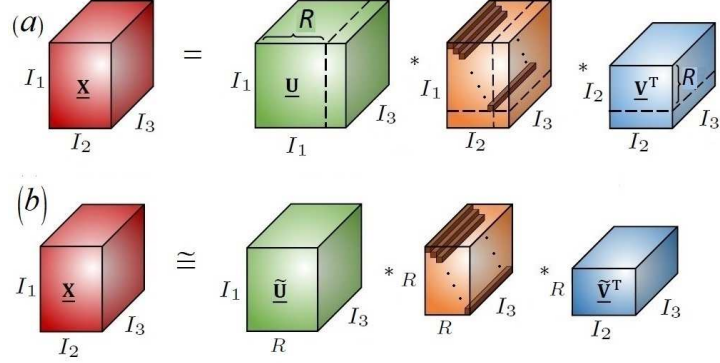


Figure 1: a) Tensor SVD (t-SVD) of the tensor $\underline{\mathbf{X}}$, b) The truncated t-SVD of the tensor $\underline{\mathbf{X}}$ for the tubal rank R [30].

the Fourier domain. In the literature, some algorithms have been developed to accelerate these computations. For example, using the idea of randomization, we can replace the classical truncated SVD with more efficient and faster approaches such as the randomized SVD [31, 16] or cross matrix approximation. Although this idea can somehow solve the mentioned computation difficulty of Algorithm 3, still we need to access all elements of the underlying data tensor. For very big data tensors where viewing the data tensor even once is very prohibitive, it is required to develop algorithms that only use a part of the data tensor at each iteration. In this paper, we follow this idea and propose an efficient algorithm for the computation of the t-SVD, which uses only a part of lateral and horizontal slices of a tensor at each iteration. This significantly accelerates the computations and in some of our simulations, we have achieved almost two orders of magnitude acceleration, which shows the performance of the proposed algorithm. To the best of our knowledge, this is the first adaptive cross algorithm developed for the computation of the t-SVD.

4. Matrix cross approximation and its adaptive version

The cross matrix approximation was first proposed in [17] for fast low-rank approximation of matrices. It provides a low-rank matrix approximation based on some actual columns and rows of the original matrix. It has been shown that a cross approximation with the maximum volume of the intersection matrix leads to close to optimal approximation [18]. The adaptive cross approximation

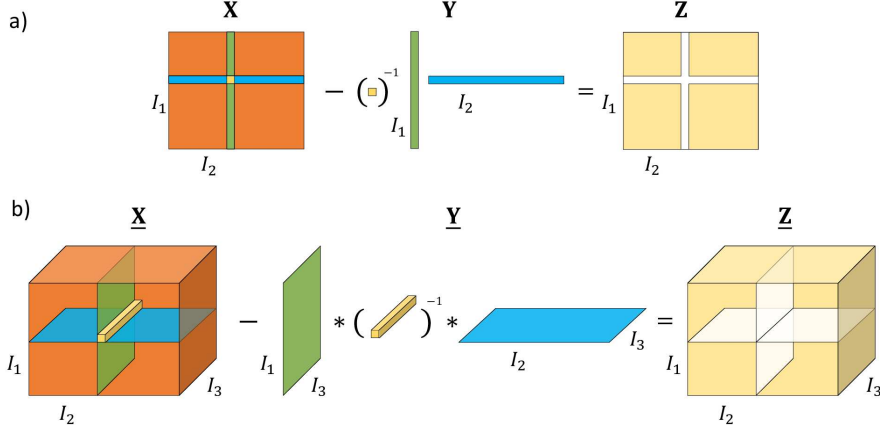


Figure 2: a) One stage of the adaptive cross matrix approximation for rank reduction. The corresponding column and row of the residual matrix \mathbf{Z} , with the same indices as the selected column and row of the original data matrix \mathbf{X} become zeros, i.e. $\text{rank}(\mathbf{X} - \mathbf{Y}) = \text{rank}(\mathbf{X}) - 1$. The rank one matrix approximation \mathbf{Y} interpolates \mathbf{X} at the selected column and row. b) One stage of the cross tubal approximation for the tubal rank reduction. The corresponding lateral and horizontal slices of the residual tensor $\underline{\mathbf{Z}}$, with the same indices as the selected lateral and horizontal slices of the original data tensor $\underline{\mathbf{X}}$ become zeros, $\text{rank}(\underline{\mathbf{X}} - \underline{\mathbf{Y}}) = \text{rank}(\underline{\mathbf{X}}) - 1$. The tubal rank one tensor approximation $\underline{\mathbf{Y}}$ interpolates $\underline{\mathbf{X}}$ at the selected lateral and horizontal slices.

Algorithm 3: The truncated t-SVD decomposition of the tensor $\underline{\mathbf{X}}$

Input : The data tensor $\underline{\mathbf{X}} \in \mathbb{R}^{I_1 \times I_2 \times I_3}$ and a target tubal rank R

Output: The truncated t-SVD of the tensor $\underline{\mathbf{X}}$

- 1 $\widehat{\underline{\mathbf{X}}} = \text{fft}(\underline{\mathbf{X}}, [], 3)$;
 - 2 **for** $i = 1, 2, \dots, \lceil \frac{I_3+1}{2} \rceil$ **do**
 - 3 $[\widehat{\underline{\mathbf{U}}}(:, :, i), \widehat{\underline{\mathbf{S}}}(:, :, i), \widehat{\underline{\mathbf{V}}}(:, :, i)] = \text{svds}(\widehat{\underline{\mathbf{X}}}(:, :, i), R)$;
 - 4 **end**
 - 5 **for** $i = \lceil \frac{I_3+1}{2} \rceil + 1, \dots, I_3$ **do**
 - 6 $\widehat{\underline{\mathbf{U}}}(:, :, i) = \text{conj}(\widehat{\underline{\mathbf{U}}}(:, :, I_3 - i + 2))$;
 - 7 $\widehat{\underline{\mathbf{S}}}(:, :, i) = \widehat{\underline{\mathbf{S}}}(:, :, I_3 - i + 2)$;
 - 8 $\widehat{\underline{\mathbf{V}}}(:, :, i) = \text{conj}(\widehat{\underline{\mathbf{V}}}(:, :, I_3 - i + 2))$;
 - 9 **end**
 - 10 $\underline{\mathbf{U}}_R = \text{ifft}(\widehat{\underline{\mathbf{U}}}, [], 3)$; $\underline{\mathbf{S}}_R = \text{ifft}(\widehat{\underline{\mathbf{S}}}, [], 3)$; $\underline{\mathbf{V}}_R = \text{ifft}(\widehat{\underline{\mathbf{V}}}, [], 3)$
-

or Cross2D algorithm [32, 33, 23, 24, 25] sequentially selects a column and a row of the original data matrix and based on them, computes a rank-1 matrix scaled by the intersection element, as stated in the following theorem, which indeed is the Gaussian elimination process.

Theorem 1. (Rank-1 deflation) Let $\mathbf{X} \in \mathbb{R}^{I_1 \times I_2}$ be a given matrix, and we select the i -th row and the j -th column with the nonzero intersection element $\mathbf{X}(i, j)$. Then the following residual matrix

$$\mathbf{Y} = \mathbf{X} - \frac{1}{\mathbf{X}(i, j)} \mathbf{X}(:, j) \mathbf{X}(i, :),$$

vanishes at the i -th row and j -th column, so $\text{rank}(\mathbf{Y}) = \text{rank}(\mathbf{X}) - 1$.

Proof. It is obvious that the j -th column and i -th row of \mathbf{Y} are zeros

$$\mathbf{Y}(:, j) = \mathbf{X}(:, j) - \frac{1}{\mathbf{X}(i, j)} \mathbf{X}(:, j) \mathbf{X}(i, j) = 0, \quad (7)$$

$$\mathbf{Y}(i, :) = \mathbf{X}(i, :) - \frac{1}{\mathbf{X}(i, j)} \mathbf{X}(i, j) \mathbf{X}(i, :) = 0. \quad (8)$$

To prove Theorem 1, we consider two cases:

1. If \mathbf{X} is of full-rank, that is, either $\mathbf{X}(:, j) \notin \text{range}(\mathbf{X}_{(:, -j)})$ or $\mathbf{X}(i, :) \notin \text{range}(\mathbf{X}_{(-i, :)})$, then it is straightforward that \mathbf{Y} has smaller rank than \mathbf{X} .
2. Otherwise, we consider the case \mathbf{X} is rank-deficient and $\mathbf{X}(:, j)$ and $\mathbf{X}(i, :)$ are non zero vectors that $\mathbf{X}(i, :) \in \text{range}(\mathbf{X}_{(-i, :)})$ and $\mathbf{X}(:, j) \in \text{range}(\mathbf{X}_{(:, -j)})$.

Without loss of generality, we assume that $\mathbf{X}(:, j)$ and $\mathbf{X}(i, :)$ are the last column and the last row of the matrix \mathbf{X} , i.e. $i = I_1$, $j = I_2$, (see illustration in Figure 3) and $\text{rank}(\mathbf{X}) < \min(I_1, I_2)$.

Since $\mathbf{X}(i, :) \in \text{range}(\mathbf{X}_{(-i, :)})$ and $\mathbf{X}(:, j) \in \text{range}(\mathbf{X}_{(:, -j)})$, there exist linear combinations such that

$$\mathbf{X}(:, j) = \begin{bmatrix} \mathbf{a} \\ c \end{bmatrix} = \begin{bmatrix} \mathbf{Z} \\ \mathbf{b}^T \end{bmatrix} \boldsymbol{\alpha}, \quad \mathbf{X}(i, :)^T = \begin{bmatrix} \mathbf{b} \\ c \end{bmatrix} = \begin{bmatrix} \mathbf{Z}^T \\ \mathbf{a}^T \end{bmatrix} \boldsymbol{\beta}, \quad (9)$$

where $\boldsymbol{\alpha} \neq 0$, $\boldsymbol{\beta} \neq 0$. This gives $c = \boldsymbol{\beta}^T \mathbf{Z} \boldsymbol{\alpha}$.

The rank-1 matrix deflation yields

$$\mathbf{Y} = \mathbf{X} - \frac{1}{c} \begin{bmatrix} \mathbf{a} \\ c \end{bmatrix} \begin{bmatrix} \mathbf{b}^T & c \end{bmatrix} = \begin{bmatrix} \mathbf{Z} - \frac{1}{c} \mathbf{a} \mathbf{b}^T & \mathbf{0} \\ \mathbf{0} & 0 \end{bmatrix}. \quad (10)$$

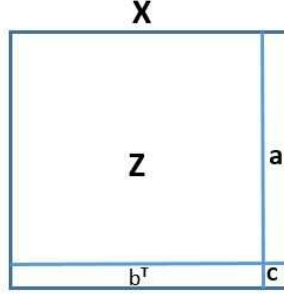


Figure 3: Partitioning the matrix \mathbf{X} for the proof of Theorem 1.

where the top-left submatrix of \mathbf{Y} has rank-1 reduction from \mathbf{Z}

$$\mathbf{W} = \mathbf{Z} - \frac{1}{c}\mathbf{a}\mathbf{b}^T = \mathbf{Z} - \frac{1}{c}\mathbf{Z}\boldsymbol{\alpha}\boldsymbol{\beta}^T\mathbf{Z}. \quad (11)$$

We next substitute \mathbf{Z} by its singular value decomposition $\mathbf{Z} = \mathbf{U}\mathbf{S}\mathbf{V}^T$, where \mathbf{S} is a diagonal matrix of positive singular values of \mathbf{Z} and consider

$$\mathbf{W} = \mathbf{U} \left(\underbrace{\mathbf{S} - \frac{1}{c}\mathbf{S}(\mathbf{V}^T\boldsymbol{\alpha})(\boldsymbol{\beta}^T\mathbf{U})\mathbf{S}}_{\mathbf{K}} \right) \mathbf{V}^T. \quad (12)$$

Assume $\mathbf{d} = \mathbf{V}^T\boldsymbol{\alpha}$ and $\mathbf{e} = \mathbf{U}^T\boldsymbol{\beta}$, then from (12), we have

$$\mathbf{K} = \mathbf{S} - \frac{\mathbf{S}\mathbf{d}\mathbf{e}^T\mathbf{S}}{\mathbf{e}^T\mathbf{S}\mathbf{d}}. \quad (13)$$

It is straightforward to see that

$$\mathbf{S}^{-1/2}\mathbf{K}\mathbf{S}^{-1/2} = \mathbf{I} - \frac{\mathbf{u}\mathbf{v}^T}{\mathbf{v}^T\mathbf{u}}, \quad (14)$$

where $\mathbf{u} = \mathbf{S}^{1/2}\mathbf{d}$ and $\mathbf{v} = \mathbf{S}^{1/2}\mathbf{e}$. Now, it is readily seen that \mathbf{K} has a zero singular value, i.e., its rank is reduced from the rank of \mathbf{S} by 1. Since the multiplication with orthogonal matrices does not change the matrix rank, the proof of the theorem is completed.

Remark 2. An alternative proof for Theorem 1 adopts the following fact proved in [34]. Given $\mathbf{X} \in \mathbb{R}^{m \times n}$ and assume $\mathbf{U} \in \mathbb{R}^{m \times k}$, $\mathbf{R} \in \mathbb{R}^{k \times k}$, and $\mathbf{V} \in \mathbb{R}^{n \times k}$. Then

$$\text{rank}(\mathbf{X} - \mathbf{U}\mathbf{R}^{-1}\mathbf{V}^T) = \text{rank}(\mathbf{X}) - \text{rank}(\mathbf{U}\mathbf{R}^{-1}\mathbf{V}^T), \quad (15)$$

if and only if there exist $\mathbf{A} \in \mathbb{R}^{n \times k}$ and $\mathbf{B} \in \mathbb{R}^{m \times k}$ such that $\mathbf{U} = \mathbf{X}\mathbf{A}$, $\mathbf{V} = \mathbf{X}^T\mathbf{B}$, and $\mathbf{R} = \mathbf{B}^T\mathbf{X}\mathbf{A}$. If we define $\mathbf{A} = \mathbf{e}_j \in \mathbb{R}^n$, $\mathbf{B} = \mathbf{e}_i \in \mathbb{R}^m$ as the j -th and i -th standard unit vectors¹. Then, we have $\mathbf{U} = \mathbf{X}\mathbf{A} = \mathbf{X}(:, j)$, $\mathbf{V} = \mathbf{X}^T\mathbf{B} = \mathbf{X}(i, :)^T$ and $\mathbf{R}^{-1} = (\mathbf{e}_i^T\mathbf{X}\mathbf{e}_j)^{-1} = \frac{1}{\mathbf{x}(i, j)}$. Now 15, demonstrates that

$$\begin{aligned} \text{rank}\left(\mathbf{X} - \frac{1}{c}\mathbf{X}(:, j)\mathbf{X}(i, :)\right) &= \text{rank}(\mathbf{X}) - \text{rank}\left(\frac{1}{c}\mathbf{X}(:, j)\mathbf{X}(i, :)\right) \\ &= \text{rank}(\mathbf{X}) - 1. \end{aligned}$$

So, this completes the proof. □

In view of Theorem 1, we see that the corresponding column and row of the residual matrix \mathbf{Y} , with the same indices as the selected column/row of the original data matrix \mathbf{X} become zero, which means that this approximation interpolates the original data matrix at the mentioned indices and reduces its rank by one order, see Figure 2 (a) for a graphical illustration of this approach. This procedure is repeated by selecting a new column and a new row of the residual matrix, so we can sequentially reduce the matrix rank and interpolate the original matrix at the new columns/rows. The adaptive cross matrix approximation method is summarized in Algorithm 4. Clearly, the breakdown can happen in Algorithm 4 if the denominator $\mathbf{u}_k(i_k)$, becomes zero. If we deal with such a case, we should select a new index i_k for which the $\mathbf{u}_k(i_k)$ is not zero. For example one can select randomly a new index, which has not been chosen previously.

5. Proposed adaptive tensor cross approximation based on the t-product

In this section, we show how to generalize the adaptive cross matrix approximation to the tensor case based on the t-product. Compared to the matrix case, instead of a column and a row, here we select a lateral slice and a horizontal slice at each iteration but the important question is how to use the intersection tube for scaling the corresponding tubal rank-1 tensor so that the tubal rank of the residual tensor is reduced one in order. We found that the inverse of the intersection tube should be used and this is proved in Theorem 3.

¹For the standard unit vector e_i , the i th element is 1 and the rest are zero.

Algorithm 4: Adaptive cross approximation algorithm (ACA) [32, 33, 23, 24, 25]

Input : A data matrix $\mathbf{X} \in \mathbb{R}^{I_1 \times I_2}$, an approximation error ϵ
Output: Low rank matrix approximation $\mathbf{X} = \mathbf{UV}$

- 1 $\mathbf{U} = 0, \mathbf{V} = 0, \mu = 0, r_0 = 0, j_1$ is a random column index
- 2 **for** $k = 1, 2, \dots, \min(I_1, I_2)$ **do**
- 3 $\mathbf{u}_k = \mathbf{E}_{k-1}(:, j_k) = \mathbf{X}(:, j_k) - \mathbf{UV}(:, j_k);$
- 4 $i_k = \arg \max_i |\mathbf{u}_k(i)|;$
- 5 $\mathbf{u}_k \leftarrow \mathbf{u}_k / \mathbf{u}_k(i_k);$
- 6 $\mathbf{v}_k^T = \mathbf{E}_{k-1}(i_k, :) = \mathbf{X}(i_k, :) - \mathbf{U}(i_k, :)\mathbf{V};$
- 7 $j_{k+1} = \arg \max_j |\mathbf{v}_k(j)|;$
- 8 $\rho^2 = \|\mathbf{u}_k\|_2^2 \|\mathbf{v}_k\|_2^2$
- 9 $\mu^2 \leftarrow \mu^2 + \rho^2 + 2 \sum_{j=1}^{k-1} \mathbf{V}(j, :) \mathbf{v}_k \mathbf{u}_k^T \mathbf{U}(:, j);$
- 10 $\mathbf{U} \leftarrow [\mathbf{U}, \mathbf{u}_k], \mathbf{V} \leftarrow [\mathbf{V}; \mathbf{v}_k^T];$
- 11 $r_k = r_{k-1} + 1;$
- 12 **if** $\rho < \epsilon \mu$ **then**
- 13 | **Break**
- 14 **end**
- 15 **end**

Theorem 3. (Tubal rank-1 deflation) Let $\underline{\mathbf{X}} \in \mathbb{R}^{I_1 \times I_2 \times I_3}$ be a given data tensor with sampled lateral and horizontal slices as $\underline{\mathbf{X}}(:, j, :)$ and $\underline{\mathbf{X}}(i, :, :)$ with the nonzero intersection tube $\underline{\mathbf{X}}(i, j, :)$. Then the residual tensor

$$\underline{\mathbf{Y}} = \underline{\mathbf{X}} - \underline{\mathbf{X}}(:, j, :) * (\underline{\mathbf{X}}(i, j, :))^{-1} * \underline{\mathbf{X}}(i, :, :), \quad (16)$$

vanishes at its i -th lateral slice and j -th horizontal slice and $\text{rank}(\underline{\mathbf{Y}}) = \text{rank}(\underline{\mathbf{X}}) - 1$.

Algorithm 5: Proposed adaptive cross tubal tensor approximation algorithm (ACTA)

Input : A data tensor $\underline{\mathbf{X}} \in \mathbb{R}^{I_1 \times I_2 \times I_3}$, an approximation error ϵ
Output: Low tubal rank tensor approximation $\underline{\mathbf{X}} = \underline{\mathbf{U}} * \underline{\mathbf{V}}$

- 1 $\underline{\mathbf{U}} = 0, \underline{\mathbf{V}} = 0, \mu = 0, r_0 = 0, j_1$ is a random lateral slice index
- 2 **for** $k = 1, 2, \dots, \min(I_1, I_2)$ **do**
- 3 $\underline{\mathbf{u}}_k = \underline{\mathbf{E}}_{k-1}(:, j_k, :) = \underline{\mathbf{X}}(:, j_k, :) - \underline{\mathbf{U}} * \underline{\mathbf{V}}(:, j_k, :);$
- 4 $i_k = \arg \max_i \|\underline{\mathbf{u}}_k(i, j_k, :)\|_2^2;$
- 5 $\underline{\mathbf{u}}_k \leftarrow \underline{\mathbf{u}}_k * (\underline{\mathbf{u}}_k(i_k, j_k, :))^{-1};$
- 6 $\underline{\mathbf{v}}_k^T = \underline{\mathbf{E}}_{k-1}(i_k, :, :) = \underline{\mathbf{X}}(i_k, :, :) - \underline{\mathbf{U}}(i_k, :, :) * \underline{\mathbf{V}};$
- 7 $j_{k+1} = \arg \max_j \|\underline{\mathbf{v}}_k(i_k, j, :)\|_2^2;$
- 8 $\rho^2 = \|\underline{\mathbf{u}}_k\|_F^2 \|\underline{\mathbf{v}}_k\|_F^2;$
- 9 $\mu^2 \leftarrow \mu^2 + \rho^2 + 2\|\sum_{j=1}^{k-1} \underline{\mathbf{v}}(j, :, :) * \underline{\mathbf{v}}_k * \underline{\mathbf{u}}_k^T * \underline{\mathbf{u}}_k(:, j, :)\|_2^2;$
- 10 $\underline{\mathbf{U}} \leftarrow [\underline{\mathbf{U}}, \underline{\mathbf{u}}_k], \underline{\mathbf{V}} \leftarrow [\underline{\mathbf{V}}; \underline{\mathbf{v}}_k^T];$
- 11 $r_k = r_{k-1} + 1;$
- 12 **if** $\rho < \epsilon\mu$ **then**
- 13 | **break**
- 14 **end**
- 15 **end**

Proof. To prove Theorem 3, we show that the i -th row and the j -th column of each frontal slice of the residual tensor $\underline{\mathbf{Y}}$ are zero. To do this, let us consider the k -th frontal slice of the residual tensor $\underline{\mathbf{Y}}$ as $\underline{\mathbf{Y}}(:, :, k)$. In the Fourier domain, it can be represented as

$$\widehat{\underline{\mathbf{Y}}}(:, :, k) = \widehat{\underline{\mathbf{X}}}(:, :, k) - \frac{1}{\widehat{\underline{\mathbf{X}}}(i, j, k)} \widehat{\underline{\mathbf{X}}}(i, j, k) \widehat{\underline{\mathbf{X}}}(i, :, k). \quad (17)$$

In view of Theorem 1, this means that the i -th row and the j -th column of the the k -th frontal slice of the tensor $\underline{\mathbf{Y}}$ in the Fourier domain are zero and its rank is one order lower than the rank of the matrix $\widehat{\mathbf{X}}(:, :, k)$. So the i -th row and the j -th column of the all frontal slices $\underline{\mathbf{X}}(:, :, k)$, $k = 1, 2, \dots, I_3$ equal to zero. This clearly completes the proof. \square

It is not difficult to see that for second-order tensors (matrices), Equation (16) is reduced to the classical matrix cross approximation. At each iteration, we select a lateral slice and a horizontal slice and perform the scaling using the pseudoinverse of the intersection tube. The corresponding scaled tubal rank-1 tensor reduces the tubal rank of the underlying data tensor by one order. It is interesting to note that similar to the matrix case where after each iteration the corresponding selected column and row in the residual matrix become zeros, here the corresponding lateral and horizontal slices of the residual tensor vanish. So, naturally, this approximation interpolates the original tensor at the mentioned slices. This procedure can proceed with the residual tensor to reduce the tubal rank sequentially. The generalized adaptive cross tubal approximation method is outlined in Algorithm 5. In Line 10 of Algorithm 5, the new horizontal and lateral slicers are concatenated along the second and first modes, respectively. The relative error accuracy is used for the stopping criterion as $\rho \leq \epsilon\mu$ according to

$$\begin{aligned}\rho &= \|\underline{\mathbf{u}}_k * \underline{\mathbf{v}}_k^T\|_F \approx \|\underline{\mathbf{X}} - \underline{\mathbf{U}} * \underline{\mathbf{V}}\|_F, \\ \mu &= \|\underline{\mathbf{U}} * \underline{\mathbf{V}}\|_F \approx \|\underline{\mathbf{X}}\|_F,\end{aligned}$$

where $\underline{\mathbf{U}} = [\underline{\mathbf{u}}_1, \dots, \underline{\mathbf{u}}_{k-1}]$ and $\underline{\mathbf{V}} = [\underline{\mathbf{v}}_1; \dots; \underline{\mathbf{v}}_{k-1}]$. It is necessary to enforce $i_k \neq i_1, i_2, \dots, i_{k-1}$ and $j_k \neq j_1, j_2, \dots, j_{k-1}$, which means that each iteration should produce new indices (different from the others). We also remark that if the size of a frontal/lateral slice is big, one can compress it using the classical cross methods, similar to [20] where the cross approximation is used in two stages for the computation of the Tucker decomposition. Although our results so far are for third-order tensors, clearly they can be straightforwardly generalized to tensors of a higher order than three, according to [29].

6. Computational complexity

The adaptive cross tensor algorithm is efficient as it only works on a lateral slice and a horizontal slice at each iteration. The computational complexity of Algorithm 5 is $\mathcal{O}((I+J)K \log(K))$. The computational complexity of the truncated t-SVD for a tensor of the size $I \times J \times K$ is $\mathcal{O}(IJK \log(K)) + \mathcal{O}(IJK \min(I, J))$.

Besides, the truncated t-SVD needs to access and process the whole data tensor while the proposed algorithm works only on a part of the lateral slice and horizontal slices at each iteration. So, it is clearly seen that the proposed Algorithm 5 requires much less memory and computational operation than the t-SVD algorithm. This makes it applicable for decomposing large-scale tensors.

7. Experimental Results

We have used MATLAB and some functions of the toolbox

<https://github.com/canyilu/Tensor-tensor-product-toolbox>

to implement the proposed algorithm using a laptop computer with 2.60 GHz Intel(R) Core(TM) i7-5600U processor and 8GB memory. We have used two metrics, *relative error* and Peak signal-to-noise ratio (PSNR) to compare the efficiency of the proposed algorithm with the baselines. The relative error is defined as follows

$$\text{Relative error} = \frac{\|\underline{\mathbf{X}} - \underline{\mathbf{U}} * \underline{\mathbf{S}} * \underline{\mathbf{V}}^T\|_F}{\|\underline{\mathbf{X}}\|_F}.$$

The PSNR is also defined as

$$\text{PSNR} = 10\log_{10} (255^2/\text{MSE}),$$

where $\text{MSE} = \frac{\|\underline{\mathbf{X}} - \widehat{\underline{\mathbf{X}}}\|_F^2}{\text{num}(\underline{\mathbf{X}})}$. Note “num” denotes the number of parameters of a given data tensor. We mainly consider three examples. In the first example, we examine the algorithms using low-rank random data tensors. In the second example, we have used the functional based tensors. In the last example, we used the images as real-world data with application to the image completion problem.

Example 1. In this example we consider a random data tensor $\underline{\mathbf{X}} \in \mathbb{R}^{N \times N \times N}$ with exact tubal rank $R = 30$ for $N = 100, 200, \dots, 600$. To generate such a tensor, we considered two standard Gaussian tensors and orthonormalize them. Let us denote these orthogonal parts by $\underline{\mathbf{U}} \in \mathbb{R}^{N \times R \times N}$ and $\underline{\mathbf{V}} \in \mathbb{R}^{N \times R \times N}$. Then, we generate a tensor $\underline{\mathbf{S}} \in \mathbb{R}^{R \times R \times N}$ with only R nonzero diagonal tubes $\underline{\mathbf{S}}(i, i, :)$, $i = 1, 2, \dots, R$ whose elements are also standard Gaussian and build the tensor $\underline{\mathbf{X}} = \underline{\mathbf{U}} * \underline{\mathbf{S}} * \underline{\mathbf{V}}^T$, which is used in our simulations. Assume that $R = 30$ in our simulations, and set $\epsilon = 10^{-8}$ in Algorithm 5. Then, we apply the proposed algorithm to find the tubal rank and the corresponding low tubal rank approximation. We consider 100 Monte Carlo experiments and report the mean of our results (accuracy and running

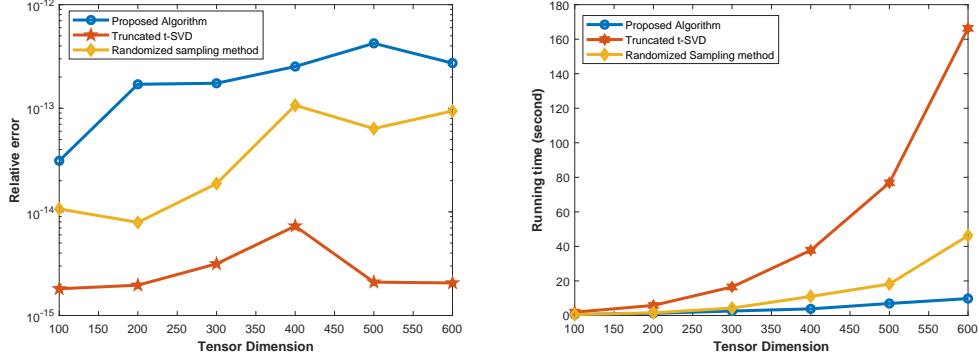


Figure 4: The running time and accuracy comparisons of the proposed algorithm and the truncated t-SVD for Example 1.

time). In all our experiments, the proposed approach retrieved the true tubal rank successfully, and this convinced us that it works well for finding the tubal rank of a tensor. Then we used the truncated t-SVD and the randomized t-SVD [22] to compute low tubal rank approximations of the underlying data tensor. The running time of the proposed algorithm, the truncated t-SVD, the randomized t-SVD are compared in Figure 4 (right). The numerical results show almost two orders of magnitude speed-up of the proposed approach compared with the truncated t-SVD algorithm, while it is also faster than the randomized t-SVD. The accuracy comparison of the algorithms is also presented in Figure 4 (left). This illustrates that the proposed algorithm can provide acceptable results in much less time than the truncated t-SVD algorithm and the randomized t-SVD.

Example 2. In this example, we apply Algorithm 5 to compute low tubal rank approximations of function based tensors. To do so, we consider the following case studies:

- Case study I: $\underline{\mathbf{X}}(i, j, k) = \frac{1}{(i^2+j^2+k^2)^{1/2}}$;
- Case study II: $\underline{\mathbf{X}}(i, j, k) = \sin(i + j + k) + \tanh(i + j + k)$;
- Case study III: $\underline{\mathbf{X}}(i, j, k) = \frac{1}{(i^5+j^5+k^5)^{1/5}}$;

where $1 \leq i, j, k \leq n$ for $n = 100, 200, \dots, 600$. It is not difficult to see that these tensors have low tubal ranks. The numerical tubal rank for case studies I, II and III for a tensor of size $100 \times 100 \times 100$ were 25, 5 and 43, respectively. However, for

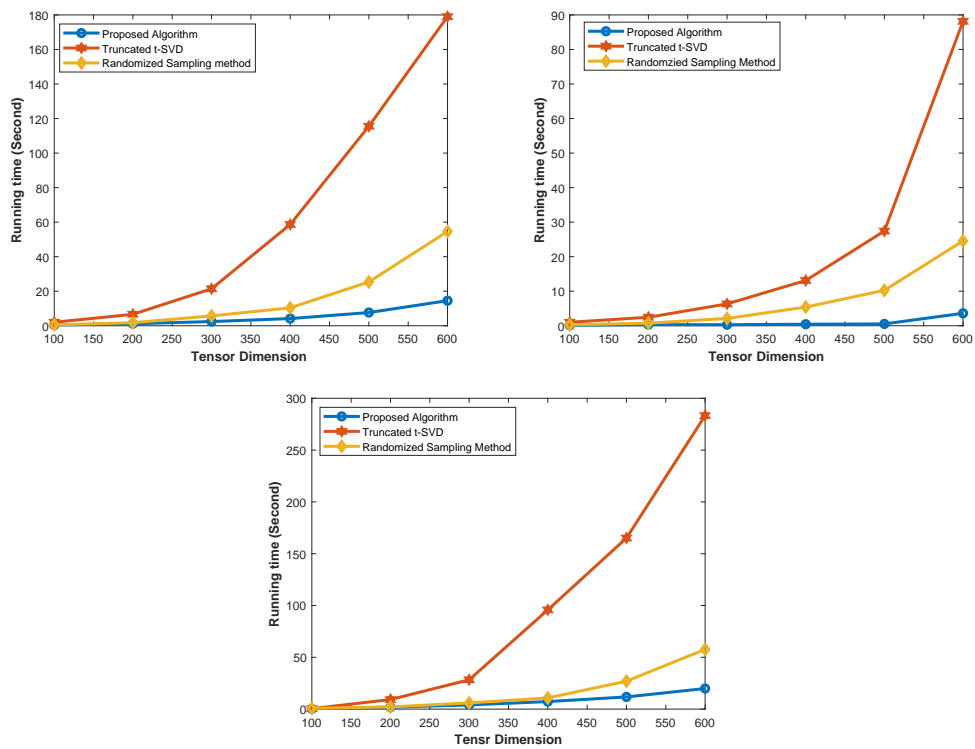


Figure 5: The running time comparison of the truncated t-SVD and the proposed algorithm for Case I (upper left), Case II (upper right) and Case III (bottom) for Example 2.



Figure 6: The original image, the available with 70% missing pixels (randomly) and the reconstructed images using the truncated t-SVD and the proposed approach for Example 3.

larger sizes the numerical tubal rank may be slightly changed. We applied the proposed approach to the mentioned data tensors in a similar way as for Example 1, to find the numerical tubal rank and the corresponding low tubal rank approximation. Here, for the case studies I, II and III, the proposed algorithm for $\epsilon = 10^{(-8)}$ gave tubal ranks 24, 5 and 42, respectively, which is very close to the true numerical tubal ranks. Then for these tubal ranks, we applied the truncated t-SVD and the randomized t-SVD to compute a low tubal rank approximation. The running time and relative errors of the solutions of the algorithms are compared in Figure 5 and Table 2, respectively. In view of Figure 5, the performance of the proposed algorithm compared with the truncated t-SVD and the randomized t-SVD is visible. These two experiments verified that the proposed approach is applicable for large-scale tensors because it works only on a small a part of the data tensor at each iteration while the classical approaches, e.g. the truncated t-SVD deals with the whole data tensor. The results in Table 2 also show that the proposed algorithm provides an approximation with almost the same accuracy as the truncated t-SVD, which is known to be the best approximation in the lease-squares sense² for the low tubal rank approximation [9].

Example 3. Application to tensor completion. In this example, we show the

²For any unitary invariant tensor norm.

Table 1: Relative errors of results obtained by the truncated t-SVD and the proposed Algorithm for Example 2.

Case study I						
Methods \ N	100	200	300	400	500	600
Truncated t-SVD [9]	1.6e-14	8.01e-13	6.9e-12	2.4e-11	5.9e-11	1.1e-10
Randomized t-SVD [22]	4.9e-14	8.4e-12	4.4e-11	1.5e-10	3.7e-10	7.7e-10
Proposed algorithm	3.1e-14	1.01e-12	3.5e-11	2.95e-10	3.2e-10	9.7e-10
Case study II						
Truncated t-SVD [9]	1.0e-15	1.6e-15	1.3e-15	1.7e-15	2.09e-15	2.5e-15
Randomized t-SVD [22]	1.2e-15	1.5e-15	1.6e-15	2.4e-15	2.06e-15	2.3e-15
Proposed algorithm	1.3e-15	1.5e-15	1.7e-15	1.8e-15	2.06e-15	2.3e-15
Case study III						
Truncated t-SVD [9]	2.7e-14	1.3e-11	1.3e-10	5.04e-10	1.1e-09	2.2e-09
Randomized t-SVD [22]	1.9e-13	1.2e-10	1.01e-09	3.5e-09	6.5e-09	1.3e-08
Proposed algorithm	5.3e-14	7.7e-11	4.7e-10	7.1e-09	3.2e-09	2.1e-08

application of the proposed adaptive algorithm for the task of tensor completion. To this end, we consider the benchmark images ‘‘Peppers’’, ‘‘Lena’’ and ‘‘House’’ that of size $256 \times 256 \times 3$ depicted in Figure 6 (left) and remove 70% of their pixels randomly shown in Figure 6 (middle). We use the Peak signal-to-noise ratio (PSNR) to compare the performance of the proposed algorithm with the benchmark algorithm. The tensor decomposition formulation (18) for the tensor completion problem is written as follows

$$\begin{aligned} \min_{\underline{\mathbf{X}}} \quad & \|\mathbf{P}_{\underline{\Omega}}(\underline{\mathbf{X}}) - \mathbf{P}_{\underline{\Omega}}(\underline{\mathbf{M}})\|_F^2, \\ \text{s.t.} \quad & \text{rank}(\underline{\mathbf{X}}) = R, \end{aligned} \quad (18)$$

where the unknown tensor $\underline{\mathbf{X}}$ to be determined, and we assume that it has low tensor rank representation, $\underline{\mathbf{M}}$ is the original data tensor and $\underline{\Omega}$ is the index of known pixels. The projector $\mathbf{P}_{\underline{\Omega}}$ is defined as follows

$$\mathbf{P}_{\underline{\Omega}}(\underline{\mathbf{X}}) = \begin{cases} \underline{\mathbf{X}}(\mathbf{i}) & \mathbf{i} \in \underline{\Omega}, \\ 0 & \mathbf{i} \notin \underline{\Omega}, \end{cases}$$

where $\mathbf{i} = (i_1, i_2, \dots, i_N)$ is an arbitrary multi-index with $1 \leq i_n \leq I_n$, $n = 1, 2, \dots, N$. Here, different kinds of tensor ranks and associated tensor decompositions can be considered in the formulation (18). The solution to the minimization problem (18) can be approximated by the following iterative procedure

$$\underline{\mathbf{Y}}^{(n)} = \mathcal{L}(\underline{\mathbf{X}}^{(n)}), \quad (19)$$

Table 2: Running time (second) and PSNR of the constructed images using the truncated t-SVD and the proposed Algorithm for Example 3, Time (s) and PSNR (dB).

	Peppers		Lena		House	
	Time	PSNR	Time	PSNR	Time	PSNR
Truncated t-SVD [9]	55.03	27.74	45.2	27.36	61.94	28.05
Randomized t-SVD [22]	10.12	27.55	11.23	27.40	10.83	29.40
Proposed algorithm	7.60	27.55	8.34	27.46	7.27	29.59

$$\underline{\mathbf{X}}^{(n+1)} = \underline{\mathbf{\Omega}} \circledast \underline{\mathbf{Y}}^{(n)} + (\underline{\mathbf{1}} - \underline{\mathbf{\Omega}}) \circledast \underline{\mathbf{Y}}^{(n)}, \quad (20)$$

as described in [35] to complete the unknown pixels where \mathcal{L} is an operator, which computes a low-rank tensor approximation of the data tensor $\underline{\mathbf{X}}^{(n)}$, $\underline{\mathbf{1}}$ is a tensor whose all components are equal to one and \circledast is the Hadamard (elementwise) product. For the low-rank computations in the first step (19), we apply the proposed Algorithm 5 with a given number of iterations and not a given tolerance to find the lateral and horizontal slice indices and compute the approximation $\underline{\mathbf{C}} * \underline{\mathbf{U}} * \underline{\mathbf{R}}$ where $\underline{\mathbf{U}} = \underline{\mathbf{C}}^\dagger * \underline{\mathbf{X}} * \underline{\mathbf{R}}^\dagger$ and $\underline{\mathbf{C}}$, $\underline{\mathbf{R}}$ are the sampled lateral and horizontal slices, respectively. The tubal rank $R = 70$, was used in our computations. Beside applying the proposed algorithm, we also used the truncated t-SVD and the randomized t-SVD in our computations. The reconstructed images using the proposed approach and the truncated t-SVD are displayed in Figure 6 (bottom). The running time required to compute these reconstructions and also their PSNR are reported in Table 2. The results in Table 2 and Figure 6, clearly illustrate that the proposed adaptive algorithm provides comparable results in much less running time. This clearly shows the feasibility and efficiency of the proposed algorithm for fast tensor completion task.

Example 4. Application to PEdesTrian Attribute Recognition task. In this experiment, we show an application of the proposed method for the Pedestrian Attributes Recognition (PAR) task [36]. We consider the PEdesTrian Attribute dataset (PETA) dataset [37], which was widely used in the literature for the PAR problem. It includes 8705 different persons in the 19000 pedestrian images, which have 65 attributes (61 binary and 4 multi-class). Although the images are not all the same size, we resize them in this experiment to $256 \times 128 \times 3$. We only take into account 1012 images and construct a fourth-order tensor with the size $256 \times 128 \times 3 \times 1012$ and reshape it into a third-order tensor with the size

$256 \times 384 \times 1012$. With an error bound of $\epsilon = 0.1$, we applied the suggested approach to the above dataset to determine the relevant tubal-rank. The truncated t-SVD of the underlying dataset was then computed for this tubal-rank. The reconstructed images that were obtained by them for two random samples using the proposed algorithm and compared to the truncated t-SVD are shown in Figure 7. Here we achieved $\times 5$ speed-up compared to the truncated t-SVD. The results unequivocally show that the suggested technique can produce similar results in less computational time. Additionally, the Attribute-specific Localization (ASL) model [38], an effective deep neural network (DNN), was taken into account as it had provided cutting-edge results for the PAR problem. In order to create a lightweight model with fewer parameters and complexity [39], we first compressed the underlying convolution layers in the ASL model using the Error Preserving Correction-CPD [40] and the SVD. As our test datasets, we also compressed 30% of the PETA dataset’s images using Algorithm 5 (for $\epsilon = 0.1, 0.2$, and 0.3) and compared the ASL model’s performance in identifying pedestrian features in the compressed and original images. Table 3 displays the experiment’s outcomes. We see that the light-weight model’s accuracy for both the original and compressed images is quite similar. It should be noted that the model was not trained on compressed photos, though one may do so to improve recognition accuracy. As a result, this concept may be applied to Internet of Things (IoT) applications where tremendous amounts of data in various shapes and formats are generated (for example, image sensors embedded in mobile cameras produce enormous amounts of data in the form of higher-resolution photographs and videos). Here, it is fundamental to install compacted DNNs and portable DL models on the edge of the IoT network, along with having fast data communication for real-time applications (denoising, defogging, deblurring, segmentation, target detection, and recognition). Using the suggested method, we may use the compressed form of the data in these applications.

8. Conclusion and future works

In this work, we proposed an adaptive tubal tensor approximation algorithm for the computation of the tensor SVD. The proposed algorithm can estimate the tubal rank of a tensor and provide the corresponding low tubal rank approximation. The experimental results verified the feasibility of the proposed algorithm. Our future work will be developing a blocked version of the proposed adaptive tubal tensor algorithm. The block version can be further improved using the parallel hierarchical strategy [41] and we will investigate this in future works. In the



Figure 7: Comparing the original images and their compressed forms by the proposed algorithm and the truncated t-SVD for Example 4.

Table 3: Comparing the running times (second) and relative errors achieved by the proposed algorithm and the Truncated t-SVD [9] with original accuracy **0.8887** for Example 4.

$\epsilon = 0.3$		
Algorithms	Running Time (s)	Recognition accuracy
Truncated t-SVD [9]	236.45	85.86%
Proposed algorithm	45.56	84.36%
$\epsilon = 0.2$		
Truncated t-SVD [9]	196.45	87.21%
Proposed algorithm	35.97	86.16%
$\epsilon = 0.1$		
Truncated t-SVD [9]	150.32	88.42%
Proposed algorithm	27.12	87.21%

matrix case, it is known that the maximum volume (maxvol) algorithm as a matrix cross approximation method provides close to optimal low-rank approximations. Generalization of the maxvol approach from the matrix case to tensors based on the t-product is our ongoing research work.

9. Acknowledgement

The authors would like to thank the editor and two reviewer reviewers for their constructive comments, which have greatly improved the quality of the paper. The work was partially supported by the Ministry of Education and Science of the Russian Federation (grant 075.10.2021.068).

10. Conflict of Interest Statement

The authors declare that they have no conflict of interest with anything.

References

- [1] I. V. Oseledets, Tensor-train decomposition, *SIAM Journal on Scientific Computing* 33 (5) (2011) 2295–2317.
- [2] L. R. Tucker, et al., The extension of factor analysis to three-dimensional matrices, *Contributions to mathematical psychology* 110119 (1964).
- [3] L. De Lathauwer, B. De Moor, J. Vandewalle, A multilinear singular value decomposition, *SIAM journal on Matrix Analysis and Applications* 21 (4) (2000) 1253–1278.
- [4] F. L. Hitchcock, Multiple invariants and generalized rank of a p-way matrix or tensor, *Journal of Mathematics and Physics* 7 (1-4) (1928) 39–79.
- [5] F. L. Hitchcock, The expression of a tensor or a polyadic as a sum of products, *Journal of Mathematics and Physics* 6 (1-4) (1927) 164–189.
- [6] L. De Lathauwer, Decompositions of a higher-order tensor in block terms—Part II: Definitions and uniqueness, *SIAM Journal on Matrix Analysis and Applications* 30 (3) (2008) 1033–1066.
- [7] Q. Zhao, G. Zhou, S. Xie, L. Zhang, A. Cichocki, Tensor ring decomposition, *arXiv preprint arXiv:1606.05535* (2016).

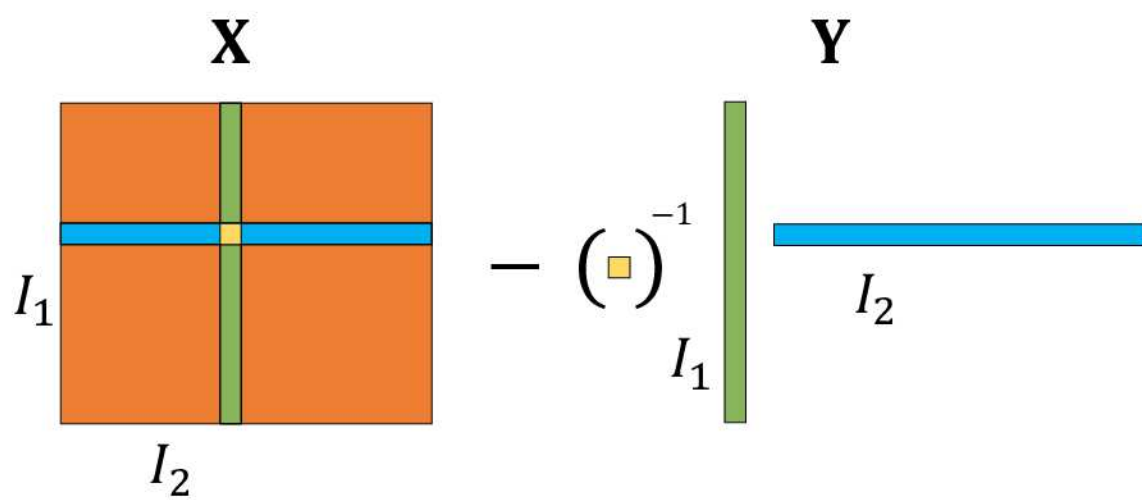
- [8] M. Espig, K. K. Naraparaju, J. Schneider, A note on tensor chain approximation, *Computing and Visualization in Science* 15 (6) (2012) 331–344.
- [9] M. E. Kilmer, C. D. Martin, Factorization strategies for third-order tensors, *Linear Algebra and its Applications* 435 (3) (2011) 641–658.
- [10] E. Newman, L. Horesh, H. Avron, M. Kilmer, Stable tensor neural networks for rapid deep learning, *arXiv preprint arXiv:1811.06569* (2018).
- [11] E. Newman, A step in the right dimension: Tensor algebra and applications, Ph.D. thesis, Tufts University (2019).
- [12] Z. Zhang, S. Aeron, Exact tensor completion using t-svd, *IEEE Transactions on Signal Processing* 65 (6) (2016) 1511–1526.
- [13] Z. Zhang, G. Ely, S. Aeron, N. Hao, M. Kilmer, Novel methods for multilinear data completion and de-noising based on tensor-svd, in: *Proceedings of the IEEE conference on computer vision and pattern recognition*, 2014, pp. 3842–3849.
- [14] S. Soltani, M. E. Kilmer, P. C. Hansen, A tensor-based dictionary learning approach to tomographic image reconstruction, *BIT Numerical Mathematics* 56 (4) (2016) 1425–1454.
- [15] M. Kilmer, L. Horesh, H. Avron, E. Newman, Tensor-tensor products for optimal representation and compression, *arXiv preprint arXiv:2001.00046* (2019).
- [16] M. W. Mahoney, et al., Randomized algorithms for matrices and data, *Foundations and Trends® in Machine Learning* 3 (2) (2011) 123–224.
- [17] S. A. Goreinov, E. E. Tyrtyshnikov, N. L. Zamarashkin, A theory of pseudoskeleton approximations, *Linear algebra and its applications* 261 (1-3) (1997) 1–21.
- [18] S. A. Goreinov, I. V. Oseledets, D. V. Savostyanov, E. E. Tyrtyshnikov, N. L. Zamarashkin, How to find a good submatrix, in: *Matrix Methods: Theory, Algorithms And Applications: Dedicated to the Memory of Gene Golub*, World Scientific, 2010, pp. 247–256.
- [19] I. Oseledets, E. Tyrtyshnikov, TT-cross approximation for multidimensional arrays, *Linear Algebra and its Applications* 432 (1) (2010) 70–88.

- [20] I. V. Oseledets, D. Savostianov, E. E. Tyrtshnikov, Tucker dimensionality reduction of three-dimensional arrays in linear time, *SIAM Journal on Matrix Analysis and Applications* 30 (3) (2008) 939–956.
- [21] C. F. Caiafa, A. Cichocki, Generalizing the column–row matrix decomposition to multi-way arrays, *Linear Algebra and its Applications* 433 (3) (2010) 557–573.
- [22] D. A. Tarzanagh, G. Michailidis, Fast randomized algorithms for t-product based tensor operations and decompositions with applications to imaging data, *SIAM Journal on Imaging Sciences* 11 (4) (2018) 2629–2664.
- [23] M. Bebendorf, Approximation of boundary element matrices, *Numerische Mathematik* 86 (4) (2000) 565–589.
- [24] M. Bebendorf, R. Grzhibovskis, Accelerating galerkin bem for linear elasticity using adaptive cross approximation, *Mathematical Methods in the Applied Sciences* 29 (14) (2006) 1721–1747.
- [25] K. Zhao, M. N. Vouvakis, J.-F. Lee, The adaptive cross approximation algorithm for accelerated method of moments computations of emc problems, *IEEE transactions on electromagnetic compatibility* 47 (4) (2005) 763–773.
- [26] O. Rojo, H. Rojo, Some results on symmetric circulant matrices and on symmetric centrosymmetric matrices, *Linear algebra and its applications* 392 (2004) 211–233.
- [27] C. Lu, J. Feng, Y. Chen, W. Liu, Z. Lin, S. Yan, Tensor robust principal component analysis with a new tensor nuclear norm, *IEEE transactions on pattern analysis and machine intelligence* 42 (4) (2019) 925–938.
- [28] M. E. Kilmer, K. Braman, N. Hao, R. C. Hoover, Third-order tensors as operators on matrices: A theoretical and computational framework with applications in imaging, *SIAM Journal on Matrix Analysis and Applications* 34 (1) (2013) 148–172.
- [29] C. D. Martin, R. Shafer, B. LaRue, An order-p tensor factorization with applications in imaging, *SIAM Journal on Scientific Computing* 35 (1) (2013) A474–A490.

- [30] S. Ahmadi-Asl, An efficient randomized fixed-precision algorithm for tensor singular value decomposition, *Communications on Applied Mathematics and Computation* (2022) 1–20.
- [31] N. Halko, P.-G. Martinsson, J. A. Tropp, Finding structure with randomness: Probabilistic algorithms for constructing approximate matrix decompositions, *SIAM review* 53 (2) (2011) 217–288.
- [32] D. Savostyanov, Polilinear approximation of matrices and integral equations, Ph. D. dissertation, Dept. Math., INM RAS, Moscow, Russia (2006).
- [33] E. Tyrtysnikov, Incomplete cross approximation in the mosaic-skeleton method, *Computing* 64 (4) (2000) 367–380.
- [34] M. T. Chu, R. E. Funderlic, G. H. Golub, A rank–one reduction formula and its applications to matrix factorizations, *SIAM review* 37 (4) (1995) 512–530.
- [35] S. Ahmadi-Asl, M. G. Asante-Mensah, A. Cichocki, A.-H. Phan, I. Osleedets, J. Wang, Cross tensor approximation for image and video completion, arXiv preprint arXiv:2207.06072 (2022).
- [36] X. Wang, S. Zheng, R. Yang, A. Zheng, Z. Chen, J. Tang, B. Luo, Pedestrian attribute recognition: A survey, *Pattern Recognition* 121 (2022) 108220.
- [37] Y. Deng, P. Luo, C. C. Loy, X. Tang, Pedestrian attribute recognition at far distance, in: *Proceedings of the 22nd ACM international conference on Multimedia*, 2014, pp. 789–792.
- [38] C. Tang, L. Sheng, Z. Zhang, X. Hu, Improving pedestrian attribute recognition with weakly-supervised multi-scale attribute-specific localization, in: *Proceedings of the IEEE/CVF International Conference on Computer Vision*, 2019, pp. 4997–5006.
- [39] A. Jha, D. Ermilov, K. Sobolev, A. H. Phan, S. Ahmadi-Asl, N. Ahmed, I. N. Junejo, Z. AL Aghbari, T. M. S. B. Shamsa, A. M. Khedr, A. Cichoki, Pedestrian attribute recognition using lightweight attribute specific localization, Submitted (2023).
- [40] A.-H. Phan, P. Tichavský, A. Cichocki, Error preserving correction: A method for cp decomposition at a target error bound, *IEEE Transactions on Signal Processing* 67 (5) (2018) 1175–1190.

- [41] Y. Liu, W. Sid-Lakhdar, E. Rebrova, P. Ghysels, X. S. Li, A parallel hierarchical blocked adaptive cross approximation algorithm, *The International Journal of High Performance Computing Applications* 34 (4) (2020) 394–408.

a)



b)

